Journal of Medicinal Chemistry



Article

# Molecular Modeling of Wild-Type and D816V c-Kit Inhibition Based on ATP-Competitive Binding of Ellipticine Derivatives to Tyrosine Kinases

Jrmie Vendme, Sbastien Letard, Frdric Martin, Fedor Svinarchuk, Patrice Dubreuil, Christian Auclair, and Marc Le Bret

*J. Med. Chem.*, **2005**, 48 (20), 6194-6201• DOI: 10.1021/jm050231m • Publication Date (Web): 07 September 2005



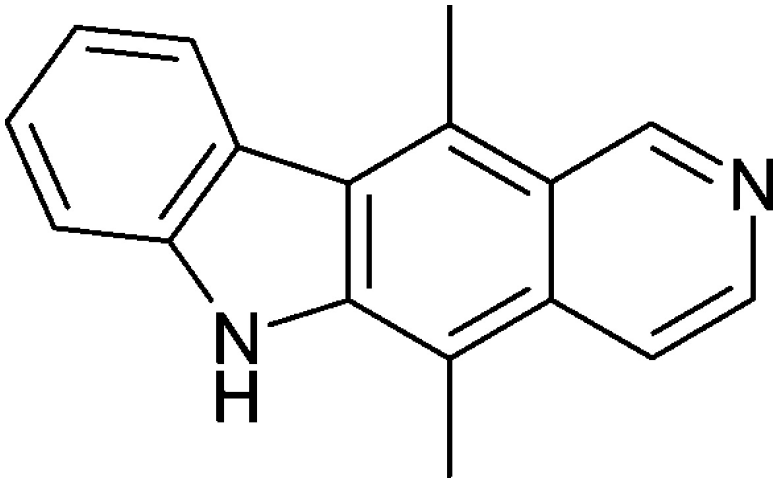


## More About This Article

Additional resources and features associated with this article are available within the HTML version:

- Supporting Information
- Links to the 2 articles that cite this article, as of the time of this article download
- Access to high resolution figures
- Links to articles and content related to this article
- Copyright permission to reproduce figures and/or text from this article

View the Full Text HTML



Journal of Medicinal Chemistry is published by the American Chemical Society. 1155 Sixteenth Street N.W., Washington, DC 20036

# Molecular Modeling of Wild-Type and D816V c-Kit Inhibition Based on ATP-Competitive Binding of Ellipticine Derivatives to Tyrosine Kinases

Jérémie Vendôme,[+] Sébastien Letard,[‡] Frédéric Martin,[§] Fedor Svinarchuk,[§] Patrice Dubreuil,[‡] Christian Auclair,[+] and Marc Le Bret*,[+]

*CNRS UMR-8113, Laboratoire de Biotechnologies et Pharmacologie génétique Appliquée (LBPA) Ecole Normale Supérieure de Cachan, 61 avenue du Président Wilson, 94235 Cachan, France, CNRS UMR-8113, LBPA, Institut Gustave Roussy, PRII, 39 rue Camille Desmoulins, 94805 Villejuif, France, and INSERM U119, Institut de Cancérologie et d'Immunologie, 27 Boulevard Lei Roure, 13009 Marseille, France*

*Received March 14, 2005*

The D816V activating mutation of the c-Kit kinase domain often causes human mastocytosis. Although inhibitors of wild-type c-Kit are known (e.g. STI-571), they are at least 10 times less active against the c-Kit mutant. Several derivatives of ellipticine (5,11-dimethyl-6*H*-pyrido-[3,4-*b*]carbazole), substituted at positions 1, 2, 9, and 11, were found to inhibit purified D816V and wild-type c-Kit kinase domains with comparable potencies by competing with ATP binding. We investigated the difference between these inhibitors by modeling the D816V mutation in crystal structures of inactive and active c-Kit. Molecular dynamics simulations strongly suggested that the D816V point mutation shifts the conformational equilibrium of c-Kit kinase domain toward the active conformation. All ellipticine compounds were subsequently docked to the D816V mutant c-Kit model. The model provides possible explanations for the structure−activity relationships observed among ellipticine compounds, resulting in new insights into D816V c-Kit mutant inhibition.

## Introduction

Receptor tyrosine kinases (RTKs) regulate the signaling pathways that control cell growth and proliferation.[1] The α and *β* receptors of the platelet-derived growth factor (PDGFR-α and PDGFR-*β*), the colony-stimulating factor-1 receptor (CSF-1, formerly c-Fms), and the stem cell factor (SCF) receptor c-Kit (or CD117 antigen) all belong to the type III RTK family.[2] Type III RTK members consist of an extracellular ligand-binding domain comprising five immunoglobulin-like repeats, a single transmembrane domain, and a cytoplasmic domain composed of a short juxtamembrane domain and the tyrosine kinase domain.

c-Kit plays a key role in mast cell survival, differentiation, maturation, and function as well as in the differentiation of melanocytes and germ cells.[3,4] The binding of SCF to the extracellular immunoglobulin-like domains of c-Kit[4] results in the homodimerization of c-Kit. This then trans-autophosphorylates specific tyrosine residues, such as Tyr 568 and Tyr 570 of the juxtamembrane domain.[5−7] This phosphorylated, active form of c-Kit binds intracellular substrates and phosphorylates them, thereby triggering multiple signaling pathways.[2,8]

Many mutations in the gene encoding the human proto-oncogene, c-Kit, are associated with highly malignant cancers. In-frame deletions affecting the negative regulatory juxtamembrane domain are associated with gastrointestinal stromal tumors.[9−11] Point mutations in the kinase domain are associated with human germ cell tumors and sporadic adult human mastocytosis.[12,13] The D816V mutation is observed in most patients with known mastocytosis.[14] Both deletions and point mutations result in the constitutive activation of c-Kit in the absence of ligand binding. The precise mechanism of action of the mutations is still unknown. Inhibitors of c-Kit, and particularly of mutated c-Kit, would have great value in cancer treatments. However, the available tyrosine kinase inhibitors, such as STI-571[15,16] (Gleevec), are only effective against wild-type c-Kit and c-Kit that has been mutated in the juxtamembrane domain and are not effective against c-Kit that has been mutated in the kinase domain.[10,17,18]

The antitumoral properties of derivatives of the alkaloid ellipticine (5,11-dimethyl-6*H*-pyrido[4,3-*b*]carbazole) have been attributed to three mechanisms. First, the planar cation intercalates between the DNA base pairs[19−21] with a high affinity and can interfere with DNA replication or DNA transcription. Second, ellipticine derivatives can induce breaks in DNA that has been extracted from cells.[21] This second mechanism involves topoisomerase II, an enzyme that makes transient DNA double-strand breaks and therefore changes DNA topology. This process is very useful in DNA transcription, DNA replication, and chromosome segregation. The topoisomerase II enzymes maintain the integrity of the transiently cleaved DNA by covalently bonding, through phosphotyrosyl bonds, between a tyrosine residue at the catalytic site of the dimeric enzyme and the newly created DNA 5′ termini. These transient, cleavable complexes are stabilized by topoisomerase II poisons such as the ellipticine derivatives.[22] The ellipticine-stabilized cleavable complexes are DNA sequence specific, having a thymine present at the 3′ end of the cleavage site.[23] In this mechanism, ellipticine is cytotoxic because it cleaves DNA, and recent studies have

* To whom correspondence should be addressed. Address: LBPA, ENS−Cachan, 61 avenue du Président Wilson, 94235 Cachan, France. Tél: 33-1-47-40-59-97; fax: 33-1-47-40-76-71; e-mail: mlebret@lbpa.ens-cachan.fr.
[+] LBPA Ecole Normale Supérieure de Cachan.
[§] LBPA Institut Gustave Roussy.
[‡] Institut de Cancérologie et d'Immunologie.

10.1021/jm050231m CCC: $30.25 
Published on Web 09/07/2005

shown that the process is more efficient if the DNA is made accessible by loosening the chromatin.[24] The third mechanism involves the ellipticine forming DNA adducts.[25,26]

Here, we show that ellipticine derivatives also have tyrosine kinase-inhibiting activity. Further, we show that several compounds have a similar inhibitory efficiency on both D816V mutant c-Kit and wild-type c-Kit. We use molecular modeling and molecular dynamics to study the structural effects of the D816V point mutation on the c-Kit kinase domain and the binding of ellipticine to the D816V c-Kit mutant. We also explain the different inhibitory characteristics of ellipticine compounds and STI-571 toward c-Kit and its D816V mutant and bring new insights into the D816V c-Kit mutant inhibition.

## Results and Discussion

**Biological Results. Ellipticine Derivatives Inhibit both D816V Mutant and Wild-Type c-Kit.** Previously reported tyrosine kinase inhibitors are inefficient against the D816V mutant.[17,18] In particular, STI-571 inhibits the kinase activity of both wild-type c-Kit and its juxtamembrane mutant but has no effect on the activity of the D816V mutant.[15,16]

We reproduced results showing the efficiency of STI-571 (compound **1**) on wild-type c-Kit and its inefficiency on the D816V mutant[16] (Table 1). We also measured, by kinase assays, the in vitro inhibiting potency of 10 pyridocarbazole derivatives (compounds **2**−**11**). We showed that ellipticine derivatives inhibit wild-type and D816V c-Kit with equal efficiency. Table 1 shows the compounds sorted according to inhibition potency against the kinase activity of wild-type c-Kit.

**Structure−Activity Relationship.** Of the ellipticine series, the most active compounds have a group at position 9 that can H-bond (see atom numbers in Figure 1). The −OH group was shown to be more efficient than an $-OCH_3$ group; therefore, position 9 should carry a group that can both donate and accept H-bonds. If the group can only receive H-bonds it is less active. Compounds that have substituents such as −H or −Br at position 9 cannot H-bond and are therefore inactive. Compound **7** seems to be an exception, but the presence of an extra intracyclic nitrogen may compensate for the absence of an −OH at position 9.

The addition of a chain at N2 does not seem to influence the c-Kit inhibiting activity: compounds **2** (no chain), **3** (methyl group), and **4** (diethyl-propyl-amine chain) are similarly active. This suggests that the nitrogen N2 is not directly involved in the binding to c-Kit.

The addition of a bulky *N*,*N*-diethyl-*N*′-methyl-propane-1,3-diamine chain at position 1 is significantly unfavorable for activity.

Finally, we studied the enzymatic activity at various inhibitor concentrations. For compound **3**, $V_{max}$ was not affected (Figure 2). We obtained similar results for all of the active compounds, showing that, for both the wild-type and D816V mutant c-Kit, inhibition competes with ATP. This indicates that the binding site of the ellipticine compounds studied here overlaps the ATP-binding site. Covalent linkage between the inhibitors and c-Kit is not consistent with the results shown in Figure 2.

**Table 1.** Results of Kinase Assay for the Compounds **1**−**11**[a]

| Compound formula | $IC_{50}$ for kinase activity inhibition[b] WT | D816V |
|---|---|---|
| 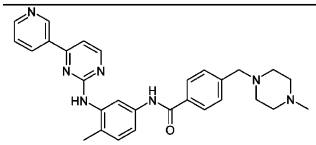 **1** (STI-571) | 0.1 | 10 |
| 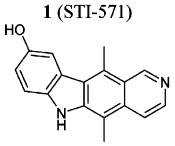 **2** | 0.4 | 0.4 |
| 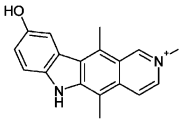 **3** | 0.4 | 0.4 |
| 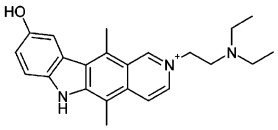 **4** | 0.45 | 0.3 |
| 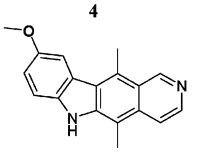 **5** | 0.8 | 0.6 |
| 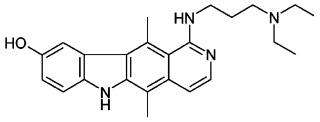 **6** | 1.4 | 1.2 |
| 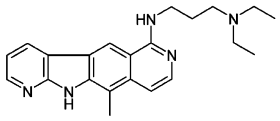 **7** | 2.3 | 1.9 |
| 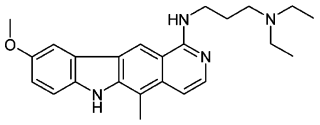 **8** | 2.5 | 2.0 |
| 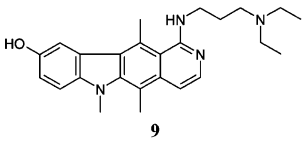 **9** | 2.5 | 3.6 |
| 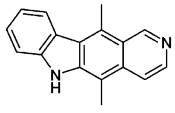 **10** | >10 | >10 |
| 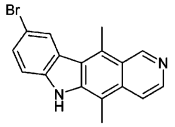 **11** | >10 | >10 |

[a] Compounds are sorted according to the kinase assay results. [b] Drug concentration ($\mu$M) at which the kinase activity of the purified kinase domain of c-Kit (either wild-type or D816V mutant) is decreased by 50%.

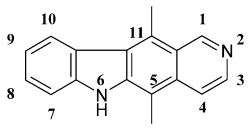


**Figure 1.** Ellipticine core atom numbering.

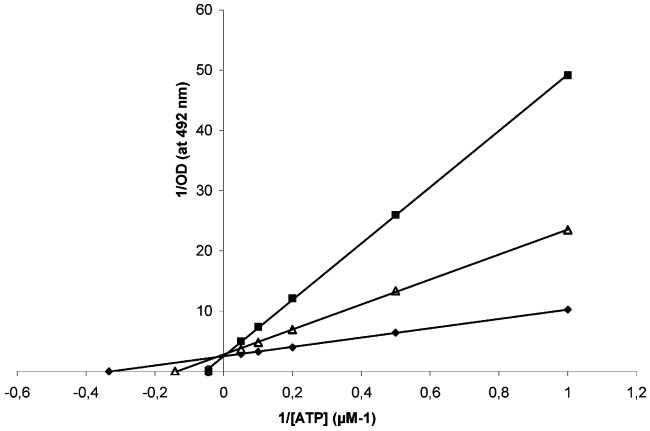


**Figure 2.** Kinetics of the c-Kit D816V inhibition by compound **3** at different concentrations: ◆ = 0 $\mu$M; △ = 0.2 $\mu$M; ■ = 0.5 $\mu$M.

**Table 2.** Results of the Kinase Inhibition Assay of Compounds **2**, **3**, and **9** on FGFR3 and PDGFR-α

| | $IC_{50}$ ($\mu$M) for kinase activity inhibition | | |
|---|---|---|---|
| tyrosine kinase | compound **2** | compound **3** | compound **8** |
| FGFR3 | 0.4 | 0.5 | 1.4 |
| PDGFR-α | 0.6 | 0.7 | 2 |

The activity of the enzyme was not affected after the incubation of c-Kit with compound **3** and the subsequent washing of the complex. This is consistent with the formation of a physical complex between ellipticine and c-Kit.

**Inhibitory Activity of Ellipticine Derivatives Against Other Tyrosine Kinases.** We tested compounds **2**, **3**, and **9** on the fibroblast growth factor receptor 3 (FGFR3) and PDGFR-α tyrosine kinases. The $IC_{50}$ values were very similar to those for c-Kit (Table 2), suggesting that ellipticine compounds have no selectivity.

We used cells that proliferate only when transfected with either D816V mutated c-Kit or wild-type c-Kit in the presence of its ligand (SCF) (see Experimental Section) to study the ex vivo activity of the compounds. In most cases, compounds that are active in vitro were also active ex vivo (Table 3). Ellipticine compounds are equally active on interleukin 3 (IL3)-mediated cell proliferation (data not shown).

This suggests that ellipticine derivatives have many targets ex vivo, which makes them highly cytotoxic. However, no known c-Kit inhibitor binds efficiently to D816V. Consequently, the in vitro affinity of ellipticine compounds for the D816V mutated enzyme is somewhat remarkable. Therefore, we studied the c-Kit kinase domain by molecular modeling to understand better the molecular basis of D816V mutant inhibition.

**Molecular Modeling.** The crystal structures of the wild-type c-Kit kinase domain have recently been determined in both its active and its inactive conformations. In the active conformation, which enables kinase activity, c-Kit is complexed with an ADP and a magnesium ion (PDB code 1PKG).[7] The juxtamembrane segment and the activation loop are in "open" positions, allowing free access to the catalytic site from the solvent. In contrast, in the inactive conformation, the c-Kit kinase activity is autoinhibited. The juxtamembrane segment enters the catalytic site and acts as a pseudosubstrate, and the activation loop obstructs the entrance to the catalytic site (PDB code 1T45)[27] (Figure 3A,B).

**Table 3.** Results of the Cell Proliferation Assay

| | $IC_{50}$ for cellular survival inhibition[a] | |
|---|---|---|
| compound | WT + SCF | D816V |
| **1** | 0.4 | 5 |
| **2** | 0.01 | 0.01 |
| **3** | 0.01 | 0.01 |
| **4** | 0.01 | 0.01 |
| **5** | 0.5 | 0.3 |
| **6** | <0.01 | <0.01 |
| **7** | 0.25 | 0.3 |
| **8** | 0.4 | 0.6 |
| **9** | nd | nd |
| **10** | 0.2 | 0.2 |
| **11** | 0.3 | 0.2 |

[a] Drug concentration ($\mu$M) that inhibits 50% of the Ba/F3 cell proliferation.

On the basis of the structures alone, it is not clear what role residue 816 plays in the constitutive activation of the enzyme because it is far from the catalytic site in the active conformation (Figure 3A). Therefore, the structures of both the wild-type and the D816V mutant c-Kit kinase domains are needed to understand the inhibition mechanism. However, no crystallographic data are available for the mutant kinase domain.

**Structural Effect of the D816V Point Mutation on the Inactive c-Kit Kinase Domain.** First, we used molecular dynamics simulations, in explicit water solvent molecules, to study the structural effects of the D816V point mutation on both c-Kit inactive and c-Kit active conformations and to determine the structure of the D816V mutant c-Kit kinase domain targeted by ellipticines. We started with the same atomic coordinates based on the crystal structure of wild-type c-Kit in its inactive conformation, but we changed the side-chain of residue 816 to a valine to simulate the wild-type and D816V mutant. In the wild-type c-Kit crystal structure, the residue Asp 816 stands close to the P-loop at the N-terminal extremity of a short $3_{10}$-helix from Ile 817 to Asp 820.[27] Here, the negatively charged Asp 816 side-chain sits in the positive potential created by the helical dipole (Figure 3C).

We monitored the folding state of the short helix by following the distance separating the CG atom of residue 816 from the N atom of residue 819. During the 6.5-ns simulation, the short helix unfolded for both structures, but it spontaneously and rapidly refolded in the wild-type structure, whereas it remained unfolded in D816V mutated structure (Figure 3D).

This confirmed the stabilizing role of the residue Asp 816 and further confirmed that an initial effect of the D816V point mutation is the destabilization of the short $3_{10}$-helix. However, we did not observe the final consequences of the short helix unfolding because few other structural changes occurred during the simulation. The numerous interactions of the juxtamembrane segment with the activation loop, the C-helix, and the P-loop probably slow the dynamics of the deformation of the

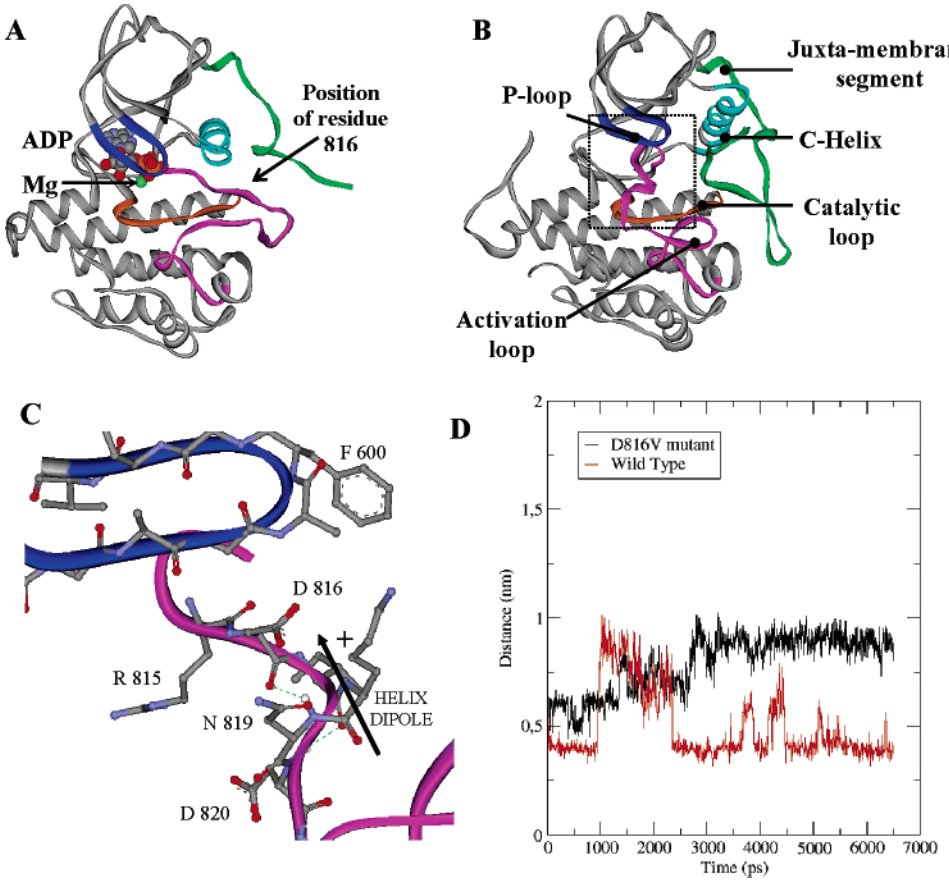


**Figure 3.** (A) and (B) represent the crystal structures of the wild-type c-Kit kinase domain in its active (PDB code 1PKG)[7] and its inactive (PDB code 1T45)[27] conformations, respectively. The important functional parts of the kinase domain are colored: the juxtamembrane segment is shown in green, the P-loop is shown in blue, the activation loop is shown in magenta, the catalytic loop is shown in orange, and the control helix is shown in cyan. In the active conformation (A) the position of the ADP and the magnesium ion indicates the ATP-binding pocket. The juxtamembrane segment and the activation loop conformations are considerably changed in the inactive conformation, making the ATP-binding pocket inaccessible. (C) Detail of the environment surrounding the Asp 816 residue in the inactive conformation (B). (D) Interatomic distance between the CG atom of residue 816 and the N atom of residue 819 of the helix, during the 6.5-ns molecular dynamics simulation, in wild-type c-Kit (red) and its D816V mutant (black).

activation loop when going from the inactive to the active conformation. To eliminate this effect and be able to observe the consequences of the short helix unfolding during a reasonable simulation time, we simulated the departure of the juxtamembrane segment by simply deleting it from the starting structures and reran the simulations. In the absence of the juxtamembrane segment, the activation loop was very mobile in the D816V mutant compared to the wild-type. However, the final D816V structure was still far from the active conformation, probably because such a large conformation change requires longer simulation times.

**Structural Effect of the D816V Point Mutation on the Active c-Kit Kinase Domain.** We explored, by molecular dynamics, the effect of the D816V mutation on the c-Kit active conformation starting from the crystal structure coordinates of the active conformation of wild-type c-Kit. Again, the only difference was the nature of the residue 816 side-chain.

We found that both structures were stable during the dynamics. The D816V point mutation had very little structural effects on the kinase domain, especially in the catalytic site area, which is a long distance from the residue 816 position.

Our study strongly suggests that the D816V point mutation moves the conformational equilibrium of c-Kit toward the active conformation. Therefore, the constitutive activation of the D816V mutant would be a result of the destabilization of the inactive conformation. The D816V mutation does not affect the active conformation.

**Pharmacological Consequences.** According to the above results, the D816V mutant constitutively adopts an active conformation very similar to the wild-type active conformation. Consequently, any potential D816V c-Kit mutant inhibitor should target the active conformation.

STI-571 binds to the inactive conformation[27] (Figure 4A). It can be seen from the docking of compound **2** to the D816V c-Kit model (Figure 4B) that the docking site overlaps the ATP-binding site (Figure 3A). It appears that the binding modes of ellipticine derivatives and STI-571 are very different: they target very different conformations.

This may explain why inhibitors such as STI-571 that selectively bind the inactive conformation[27] cannot bind the active conformation of the mutated enzyme (Figure 4).

Moreover, we have shown that both wild-type and D816V c-Kit can adopt very similar active conformations, particularly in the catalytic site area, which is a long distance from residue 816 (Figure 4B). Therefore, the compounds that are active against the D816V c-Kit

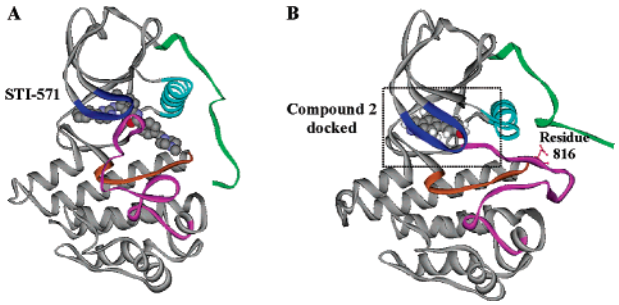


**Figure 4.** (A) In the crystal structure, STI-571 binds to the characteristic inactive conformation of c-Kit (PDB code 1T46).[27] (B) For comparison, the docked position of compound **2** in the D816V c-Kit model.

mutant should be active against the wild-type c-Kit, consistent with the results in Table 1.

Therefore, we used a crystal structure very similar to the active conformation of wild-type c-Kit to search for the ellipticine binding site on the mutant.

**Ellipticine Binding Mode Determination.** All of the compounds listed in Table 1 were docked on our model of the D816V c-Kit mutant. Because ellipticine compounds have been shown to be ATP-competitive inhibitors, we restricted our search to the catalytic site area.

We can group the compounds into three groups according to their binding mode. First, all of the active compounds (**2**, **3**, **4**, and **5**) docked very similarly in a site that is made favorable by three conserved interactions (Figure 5A,B): the −NH at position 2 is an H-bond donor to the −OH of Thr 670, and the −OH at position 9 is an H-bond donor to the carboxylic of Glu 640 and an H-bond acceptor from the ammonium group of Lys 623. Second, the docking of the inactive compounds (**10** and **11**) occurred at the same position but in a conformation (the planar cycle core flipped) different from that of the active compounds in which the three interactions are clearly impossible (Figure 5C). Third, the weakly active compounds (**6**, **7**, **8**, and **9**) (Figure 5D) bound less specifically at the same site, as we found several other binding sites for each of these compounds. The long, bulky substituent of these compounds at position 1 makes specific binding less favorable. The pyrrolic nitrogen was not involved in the binding for some of these sites. Also, the binding mode that we found for compound **7** can explain its activity, which, despite lacking an −OH at position 9, has an activity similar to compounds **6** and **8**. We found that the N7 interacts with the backbone nitrogen atom of Cys 673, compensating for the lack of 9-OH.

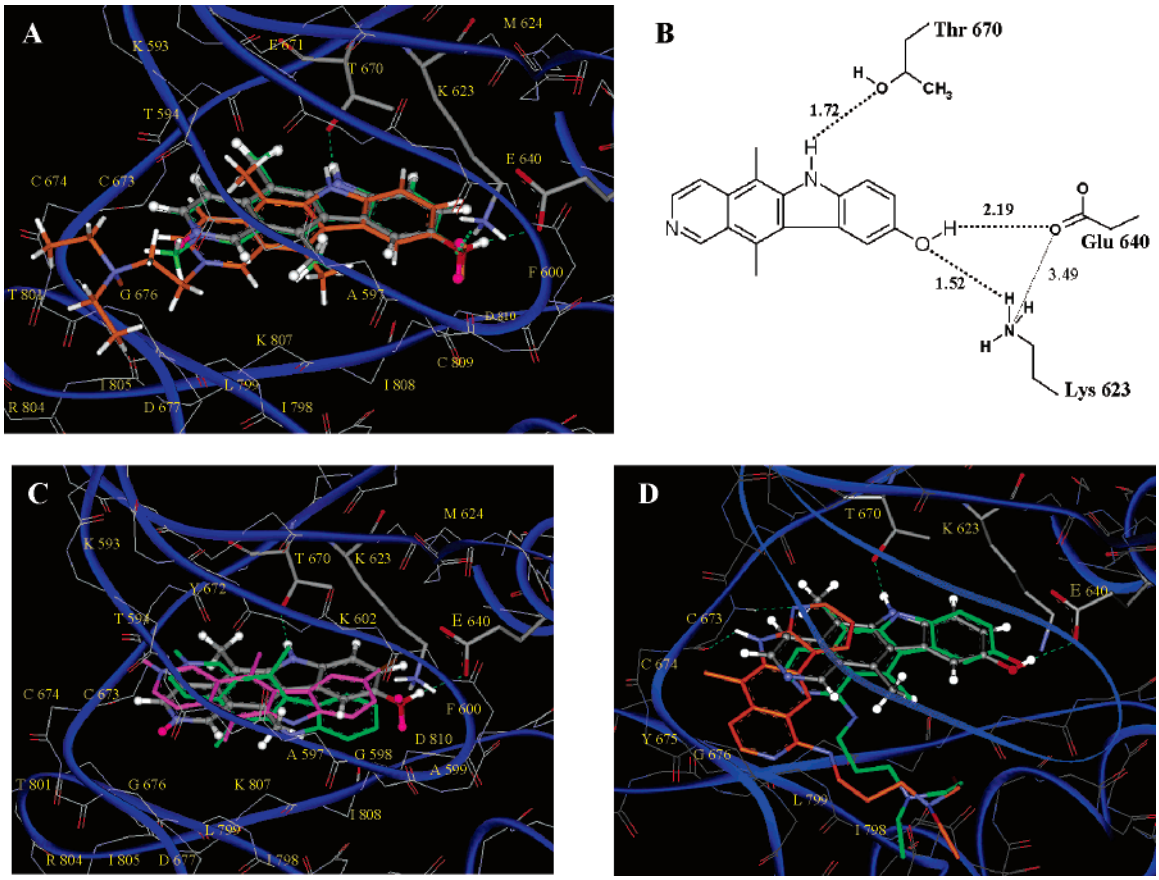


**Figure 5.** (A) Detail of the docked position of the most active compounds (compound is **2** shown in gray, **3** is shown in green, and **4** is shown in orange). Conserved interactions are represented in dashed lines. (B) Map of the main interactions for compound **2**. (C) and (D) Docked position of the less-active compounds. The docked position of the active compound **2** is recalled (ball-and-sticks representation, shown in gray) for comparison. (C) The cycles of compounds **10** (green) and **11** (magenta) are flipped in comparison with the cycle of compound **2**. These positions are less favorable because the "conserved interactions" previously described (B) are no longer possible. (D) For compounds **6** (green), **7** (orange), **8**, and **9**, having the same tail in position 1, the dockings revealed several possible binding sites. In particular, for some binding sites, the N6 is not involved in any interaction (compound **9**, not shown in the picture). It also shows how N7 can be involved in the binding of compound **7** (orange) and compensate for the lack of the 9-OH.

Furthermore, the binding mode that we found for the active compounds can explain the structure−activity relationships observed in the kinase assays (Figure 5B).

As expected, the hydroxyl group at position 9 is crucial in this binding mode because it is involved in two H-bonds (with the amine group of Lys 623 and with the carboxy group of Glu 640). Compound **5**, which has a 9-methoxy group, would make only one H-bond (with the amine group of Lys 623), resulting in a reduction in activity.

In this binding mode, the N2 atom of each compound does not directly interact with anything, and it sits within an unoccupied area. Therefore, the presence of methyl (compound **3**) or a diethyl-propyl-amine chain (compound **4**) did not change the binding site.

The protonation state at position 2 of all the compounds that were not substituted at this position (**2**, **5**, **6**, **7**, **8**, **9**, **10**, and **11**) was unknown. Therefore, we docked both forms on the D816V mutant. We found that the protonation state of the N2 did not cause any significant change in the observed sites.

## Conclusion

We have shown that the ellipticines inhibit c-Kit in vitro by competing with ATP. They inhibit the wild-type c-Kit as well as the D816V mutated enzyme responsible for mastocytosis. Our modeling shows that the D816V mutant constitutively adopts an active conformation very similar to the crystallized wild-type active conformation. This explains the inefficiency of inhibitors that target the inactive conformation of the D816V mutated c-Kit, such as STI-571. Furthermore, we also found a binding site for ellipticine derivatives that can explain the structure−activity relationships observed in the kinase assays. Finally, although our ellipticine derivatives, as they stand, cannot be used as a long-term treatment for the symptomatic effects of mastocytosis because of their cytotoxicity, they have given us a better understanding of D816V c-Kit mutant inhibition. This model is currently being used to design new compounds.

## Experimental Section

**Chemical Compounds.** Compounds were tested from freshly prepared solutions. STI-571 (compound **1**) was kindly provided by E. Buchdunger (Novartis Pharma, Basel, Switzerland). Ellipticine derivatives **2**, **3**, **4**, **5**, **10**, and **11** were readily available from our laboratory. Compounds **2** and **11** were from a series of compounds[19] that led to the antitumor compound **3**, known as Celiptium, and then led to compound **4**.[28] Compounds **6**, **7**, **8**, and **9**, containing a 1-alkylamino chain, are similar to the compounds previously described[29] and belong to the Chimiothèque Curie-CNRS, UMR 176 CNRS, Institut Curie, Bat 110, 91405 Orsay, France.

**Kit WT and Kit-D816V Protein Purification.** The baculovirus expression system, culture media, reagents, and vectors were purchased from InVitrogen and SIGMA. Oligonucleotides were purchased from Gibco. The affinity-purified, HRP goat anti-rabbit IgG was purchased from Jackson Laboratories, the anti-phosphotyrosine antibodies were purchaed from SIGMA, and the His-Tag monoclonal antibody was purchased from Novagen. Standards for gel electrophoresis were purchased from MBI Fermentas. Sepharose Q Fast Flow and HiTrap Chelating HP were purchased from Amersham Pharmacia Biotech AB.

**Construction of Recombinant Baculovirus Vectors.** The wild-type and D816V c-Kit was a gift from Dr. Jacobson (AMGEN). Both the wild-type and the D816V c-Kit were amplified using a PCR of the c-Kit containing a pSPOT1 vector. An amino-terminal hexahistidine tag, and BamH1 and Xba1 restriction sites were added during PCR. The PCR product was gel purified, digested, and ligated into the pGEM-T Easy (Promega) plasmid. The fidelity of inserts was confirmed by sequencing. The sequences were recloned into BamH1/Xba1 restriction sites on the pVL1393 transfer vector (Pharmingen) to express the human intracellular domain of the c-Kit receptor (amino acids 567 to 976). Sf9 cells were transfected with the BaculoGold Transfection kit from PharMingen according to the manufacturer's instructions. The recombinant baculovirus, obtained from the transfection protocol, was amplified to a titer of $>1 \times 10^8$ pfu/mL before the infections for protein expression were performed. We carried out two to three rounds of amplifications using $5 \times 10^6$ cells per 10-cm plate with 500 $\mu$L of transfection supernatant in 15 mL of TNM-FH medium. The titer was verified using serial dilution plaque assays in duplicate.

**Protein Expression and Purification.** Both wild-type and D816V c-Kit proteins were expressed and purified using similar protocols. High Five (Invitrogen) cell lines derived from *Trichoplusia ni* were propagated at 27 °C in 150-cm$^2$ flasks using Express Five serum free medium (Invitrogen). The cell density was maintained between $5 \times 10^5$ and $3 \times 10^6$ cells/mL for propagation. Protein expression was initiated by infecting High Five cells ($5 \times 10^5$ cells/mL) with recombinant baculovirus at a multiplicity of infection (MOI) of 10. Cells were pelleted 90 h after infection, washed once in the cold phosphate-buffered saline (PBS) buffer, and resuspended in a cold breaking buffer [250 mM NaCl, 10% (v/v) protease cocktail inhibitors (Invitrogene), 1 mM sodium vanadate, 1% Triton X-100, 40 mM Tris-HCl, pH 8.0]. We used 1.5 mL of the cold breaking buffer for one 150-cm$^2$ flask. The sample was lysed by sonication for 60 s by repeatedly alternating sonication for 3 s and 3 s on ice. The lysate was cleared by centrifugation at 30000g for 60 min at 4 °C, followed by filtration through a 0.22-$\mu$m MILLEX GP filter (Millipore). The proteins were purified by two successive steps of ion exchange and affinity chromatography.

**1. Ion Exchange Chromatography.** The filtered lysate was diluted to 0.150 M NaCl with milliQ water and loaded on a 4-mL Sepharose Q Fast Flow column connected to the Pharmacia FPLC system. The column was successively washed with 10 mL of 0.2 M NaCl and 0.25 M NaCl in a buffer containing 1% Triton X-100 and 20 mM Tris-HCl, pH 9.0. c-Kit protein was eluted with 10 mL of the same buffer containing 0.33 M NaCl.

**2. Affinity Chromatography.** A HiTrap Chelating HP 1-mL column (Amersham Pharmacia Biotech) loaded with $NiSO_4$ was used for affinity purification. The protein from the first purification step, in a buffer containing 0.5 M NaCl, 1% Triton X-100, and 20 mM Tris-HCl, pH 9.0, was applied to a column equilibrated with the same buffer. The column was successively washed with 5 mL of the buffer, 5 mL of the buffer with 0.05 M imidazole, and 5 mL of the buffer without Triton X-100. Bound protein was eluted with 2.5 mL of a buffer containing 0.25 M imidazole, 0.5 M NaCl, and 20 mM Tris-HCl. The purified protein was mixed with one volume of 50% glycerol and 1/1000 (v/v) of 1 M freshly prepared DTT, divided into aliquots, and stored at −80 °C. Purification was monitored by SDS−PAGE with the resulting bands visualized with Coomassie blue staining and Western blotting.

**Other Kinases.** Both the PDGFR-α and the FGFR3 enzymes were obtained from EUROMEDEX.

**Kinase Assay In Vitro.** We used an ELISA assay to assess the tyrosine kinase activity of wild-type and D816V c-Kit proteins. A 96-well microtiter plate (Immulon 2HB, ThermoLifeScience) was coated by incubation overnight with a 0.25-mg/mL solution of poly-Glu/Tyr (PGT) 1:4 polymer, rinsed twice with 250 $\mu$L of washing buffer (PBS-Tween: 10 mM phosphate-buffered saline, pH 7.4, and 0.05% Tween 20), and dried for 2 h at room temperature. Reactions were carried out by incubation for 15 min at 25 °C in a final volume of 100 $\mu$L in kinase buffer: 10 mM $MgCl_2$, 1 mM $MnCl_2$, 1 mM sodium vanadate, 1/25 (v/v) protease inhibitor cocktail (Invitrogen),

20 mM HEPES (pH 7.3), and 2.5 mg/mL of BSA. Reactions were initiated by the addition of the enzyme (with a final concentration of 10 nM) to a complete reaction mixture. Reactions were terminated by the addition of up to 10 mM EDTA. The plates were washed five times with washing buffer and the level of PGT phosphorylation was probed with a purified phosphotyrosine specific monoclonal antibody conjugated to horseradish peroxidase (HRP) (dilution factor 15 000). The plates were washed five times with washing buffer, and the color was developed with an HRP chromogenic substrate (OPD). The color was quantified by spectrophotometry at 492 nm. These data were used to determine the $IC_{50}$ [drug concentration ($\mu$M) at which the kinase activity of the purified kinase domain of c-Kit is decreased by 50%] for all tested ellipticine derivatives. For the active compounds, the inverse $1/OD^{492}$ values were plotted against 1/[ATP] for a given inhibitor concentration [I], giving $1/K_{m,app}$ as the intercept of the horizontal axis (see Figure 2). The dissociation constant of the inhibitor KI was then determined by fitting the apparent $K_{m,app}$ to [I] through $K_m/K_{m,app} = 1 + [I]/KI$.

**Cell Proliferation Assay. Cell Cultures.** The cell lines, Ba/F3 Kit and Ba/F3 human Kit D816V, have already been described.[16] They are derived from the murine IL3-dependent Ba/F3 proB lymphoid cells and transfected with human wild-type and D816V c-Kit.

The D816V c-Kit mutation made the Ba/F3 cell line proliferate independent of cytokine. Ba/F3 cells were cultivated in RMPI 1640 medium supplemented with 10% FCS, penicillin (100 UI/mL), and streptomycin (0.1 mg/mL) (all from Gibco/BRL); either 250 mg/mL of SCF or 10 mg/mL of IL3 was added to the Ba/F3 wild-type c-Kit culture. Cells were cultivated at 37 °C in a humidified atmosphere containing 5% $CO_2$.

**Cell Proliferation Assay.** The cell proliferation assay was determined by the 3-(4,5-dimethyl-thiazol-2-yl)-2,5-diphenyl-tetrazolium bromide (MTT) (Sigma) colorimetric method after 2 days of culture.

We diluted the drugs to obtain final concentrations of DMSO that did not exceed 0.5% to avoid the effect of DMSO on Ba/F3 cell proliferation. Cells were seeded in triplicate in 96-well plates, at a density of $10^4$ cells/well, in the presence of various concentrations of drug ($10^{-5}$−$10^{-10}$ M) or of DMSO. After 48 h of incubation, the percentage of growth inhibition was calculated by a comparison with DMSO-treated control cells, which provided the drug concentration that inhibits 50% of cell growth ($IC_{50}$).

**Molecular Modeling. Initial Structures.** We used the crystal structures of the c-Kit kinase domain in either its active conformation (PDB code 1PKG)[7] or its inactive conformation (PDB code 1T45)[27] as the starting points for our study. For each of these two structures, we changed the aspartate side-chain at residue 816 to a valine side-chain to simulate the D816V point mutation. The nonresolved part of the active conformation structure (Thr 752 to Leu 762) was completed on the basis of the structure of the resolved inactive conformation. Finally, we obtained four structures of the c-Kit kinase domain: active and inactive wild-type c-Kit and active and inactive mutant D816V c-Kit.

**Molecular Dynamics in Aqua.** The six simulations proceeded in the same way. The protein was embedded in a triclinic box filled with ~10 200 simple point charge (SPC) water molecules in periodic boundary conditions under a constant pressure of 1 atm and at a temperature of 310 K. We ensured the global charge neutrality by adding counterions in the box as needed: for the inactive conformation we added one $Na^+$ for the wild-type and one $Cl^-$ for the D816V mutant without the juxtamembrane domain, and for the active conformation we added one $Cl^-$ for the wild-type and two $Cl^-$ ions for the D816V mutant. Dynamic simulations were carried out with GROMACS using the GROMOS force field.[30,31] Electrostatic interactions were calculated with the particle mesh technique for Ewald sums, with a cutoff of 10 Å. We equilibrated the system by heating it so that only the water molecules were free to move, and the protein atoms were constrained (four 250-ps steps). The production phase was then run for 6.5 ns. The frames were recorded at 0.1-ps intervals.

**Dockings.** We modeled all the ellipticine derivatives tested in the biological assays. The partial charges were calculated using the partial equalization of orbital electronegativity (PEOE)[32] method in MOE. We modeled both protonated and nonprotonated forms at position 2 for each compound (except for compounds **3** and **4**, which are already substituted at position 2). We docked all the compounds on our D816V c-Kit mutant kinase model using the GOLD program. This algorithm allows ligand flexibility but keeps the protein rigid. We localized our search to 15 Å around the N atom of the Cys 673 backbone (ATP-binding pocket). No other constraint was imposed.

**Acknowledgment.** This work was supported by funds from ABscience, 3 avenue George V 75008 Paris, France. We thank Ms. Thi Tran and Bérengère Lefèvre for their excellent technical work. We thank Pr. Wolfgang Sippl for kindly providing calculation facilities. P.D. thanks La Ligue contre le Cancer for support.

## References

(1) Schlessinger, J. Cell signaling by receptor tyrosine kinases. *Cell* **2000**, *103*, 211−225.
(2) Hunter, T. Signaling- -2000 and beyond. *Cell* **2000**, *100*, 113−127.
(3) Galli, S. J.; Kitamura, Y. Genetically mast cell deficient w/w$^v$ and sl/sl$^d$ mice. Their value for the analysis of the roles of mast cells in biologic responses in vivo. *Am. J. Pathol.* **1987**, *127*, 191−198.
(4) Galli, S. J.; Zsebo, K. M.; Geissler, E. N. The kit ligand, stem cell factor. *Adv. Immunol.* **1994**, *55*, 1−96.
(5) Weiss, A.; Schlessinger, J. Switching signals on or off by receptor dimerization. *Cell* **1998**, *94*, 277−280.
(6) Huse, M.; Kuriyan, J. The conformational plasticity of protein kinases. *Cell* **2002**, *109*, 275−282.
(7) Mol, C. D.; Lim, K. B.; Sridhar, V.; Zou, H.; Chien, E. Y.; Sang, B. C.; Nowakowski, J.; Kassel, D. B.; Cronin, C. N.; McRee, D. E. Structure of a c-kit product complex reveals the basis for kinase transactivation. *J. Biol. Chem.* **2003**, *278*, 31461−31464.
(8) Lemmon, M. A.; Ferguson, K. M.; O′Brien, R.; Sigler, P. S.; Schlessinger, J. Specific and high-affinity binding of inositol phosphates to an isolated pleckstrin homology domain. *Proc. Natl. Acad. Sci. U.S.A.* **1995,** *97*, 10472−10476.
(9) Ma, Y.; Longley, B. J.; Wang, X.; Blount, J. L.; Langley, K.; Caughey, G. H. Clustering of activating mutations in c-KIT's juxtamembrane coding region in canine mast cell neoplasms. *J. Invest. Dermatol*. **1999**, *112*, 165−170.
(10) Furitsu, T.; Tsujimura, T.; Tono, T.; Ikeda, H.; Kitayama, H.; Koshimizu, U.; Sugahara, H.; Butterfield, J. H.; Ashman, L. K.; Kanayama, Y.; et al. Identification of mutations in the coding sequence of the proto-oncogene c-Kit in a human mast cell leukemia cell line causing a ligand-independent activation of c-Kit product. *J. Clin. Invest.* **1993**, *92*, 1736−1744.
(11) Hirota, S.; Isozaki, K.; Moriyama, Y.; Hashimoto, K.; Nishida, T.; Ishiguro, S.; Kawano, K.; Hanada, K.; Kurata, A.; Takeda, M.; Muhammad Tunio, G.; Matsuzawa, Y.; Kanakura, Y.; Shinomura, Y.; Kitamura, Y. Gain-of-function mutations of c-Kit in human gastrointestinal tumors. *Science* **1998**, *279*, 577−580.
(12) Liao, A. T.; Chien, M. B.; Shenoy, N.; Mendel, D. B.; McMahon, G.; Cherrington, J. M.; London, C. A. Inhibition of constitutively active forms of mutant kit by multitargeted indolinone tyrosine kinase inhibitors. *Blood* **2002**, *100*, 585−593.
(13) Tsujimura, T.; Furitsu, T.; Morimoto, M.; Isozaki, K.; Nomura, S.; Matsuzawa, Y.; Kitamura, Y.; Kanakura, Y. Ligand-independent activation of c-kit receptor tyrosine kinase in a murine mastocytoma cell line P-815 generated by a point mutation. *Blood* **1994**, *83*, 2619−2626.
(14) Nagata, H.; Okada, T.; Worobec, A. S.; Semere, T.; Metcalfe, D. D. c-Kit mutation in a population of patients with mastocytosis. *Int. Arch. Allergy Immunol.* **1997**, *113*, 184−186.
(15) Ma, Y.; Zeng, S.; Metcalfe, D. D.; Akin, C.; Dimitrijevic, S.; Butterfield, J. H.; McMahon, G.; Longley, B. J. The c-KIT mutation causing human mastocytosis is resistant to STI571 and other KIT kinase inhibitors; kinases with enzymatic site mutations show different inhibitor sensitivity profiles than wild-type kinases and those with regulatory-type mutations. *Blood* **2002**, *99*, 1741−1744.

(16) Zermati, Y.; De Sepulveda, P.; Feger, F.; Letard, S.; Kersual, J.; Casteran, N.; Gorochov, G.; Dy, M.; Ribadeau Dumas, A.; Dorgham, K.; Prizot, C.; Bieche, Y.; Vidaud, M.; Hermine, O.; Dubreuil, P. Effect of tyrosine kinase inhibitor STI571 on the kinase activity of wild-type and various mutated c-Kit receptors found in mast cell neoplasms. *Oncogene* **2003**, *22*, 660−664.
(17) Ma, Y.; Carter, E.; Wang, X.; Shu, C.; McMahon, G.; Longley, B. J. Indolinone derivatives inhibit constitutively activated KIT mutants and kill neoplastic mast cells. *J. Invest. Dermatol.* **2000**, *114*, 392−394.
(18) Longley, B. J.; Reguera, M. J.; Ma, Y. Classes of c-KIT activating mutations: proposed mechanisms of action and implications for disease classification and therapy. *Leuk. Res.* **2001**, *25*, 571−576.
(19) Le Pecq, J. B.; Nguyen-Dat-Xuong. X.; Gossi, C.; Paoletti, C. A new antitumoral agent: 9-hydroxyellipticine. Possibility of a rational design of anticancerous drugs in the series of DNA intercalating drugs. *Proc. Natl. Acad. Sci. U.S.A.* **1974**, *71*, 5078−5082.
(20) Kohn, K. W.; Waring, M. J.; Glaubiger, D.; Friedman, C. A. Intercalative binding of ellipticine to DNA. *Cancer Res.* **1975**, *35*, 71−76.
(21) Zwelling, L. A.; Michaels, S.; Kerrigan, D.; Pommier, Y.; Kohn, K. W. Protein-associated deoxyribonucleic acid strand breaks produced in mouse leukemia L1210 cells by ellipticine and 2-methyl-9-hydroxyellipticinium. *Biochem. Pharmacol.* **1982**, *31*, 3261−3267.
(22) Tewey, K. M.; Chen, G. L.; Nelson, E. M.; Liu, L. F. Intercalative antitumor drugs interfere with the breakage-reunion reaction of mammalian DNA topoisomerase II. *J. Biol. Chem.* **1984**, *259*, 9182−9187.
(23) Fosse, P.; Rene, B.; Le Bret, M.; Paoletti, C.; Saucier, J. M. Sequence requirements for mammalian topoisomerase II mediated DNA cleavage stimulated by an ellipticine derivative. *Nucleic Acids Res.* **1991**, *19*, 2861−2868.
(24) Kim, M. S.; Blake, M.; Baek, J. H.; Kohlhagen, G.; Pommier, Y.; Carrier, F. Inhibition of histone deacetylase increases cytotoxicity to anticancer drugs targeting DNA. *Cancer Res.* **2003**, *63*, 7291−7300.
(25) De Marini, D. M.; Abu-Shakra, A.; Gupta, R.; Hendee, L. J.; Levine, J. G. Molecular analysis of mutations induced by the intercalating agent ellipticine at the hisD3052 allele of *Salmonella typhimurium* TA98. *Environ. Mol. Mutagen.* **1992**, *20*, 12−18.
(26) Stiborova, M.; Breuer, A.; Aimova, D.; Stiborova-Rupertova, M.; Wiessler, M.; Frei, E. DNA adduct formation by the anticancer drug ellipticine in rats determined by 32P postlabeling. *Int. J. Cancer* **2003**, *107*, 885−890.
(27) Mol, C. D.; Dougan, D. R.; Schneider, T. R.; Skene, R. J.; Kraus, M. L.; Scheibe, D. N.; Snell, G. P.; Zou, H.; Sang, B. C.; Wilson, K. P. Structural basis for the autoinhibition and STI-571 inhibition of c-kit tyrosine kinase. *J. Biol. Chem.* **2004**, *279*, 31655−31663.
(28) Auclair, C.; Pierre, A.; Voisin, E.; Pepin, O.; Cros, S.; Colas, C.; Saucier, J. M.; Vershuere, B.; Gros, B.; Paoletti, C. Physicochemical and pharmacological properties of the antitumor ellipticine derivative 2-(diethylamino-2-ethyl)9-hydroxy ellipticinium-chloride, HCl. *Cancer Res.* **1987**, *47*, 6254−6261.
(29) Larue, L.; Rivalle, C.; Muzard, G.; Paoletti, C.; Bisagni, E.; Paoletti, J. A new series of ellipticine derivatives (1-(alkylamino)-9-methoxyellipticine). Synthesis, DNA binding, and biological properties. *J. Med. Chem.* **1988**, *31*, 1951−1956.
(30) Berendsen, H. J. C.; Van der Spoel, D.; and Van Drunen, R. GROMACS: a message-passing parallel molecular dynamics implementation. *Comput. Phys. Commun.* **1995**, *91*, 43−56.
(31) Lindahl, E.; Hess, B.; Van der Spoel, D. GROMACS: a package for molecular simulation and trajectory analysis. *J. Mol. Model.* **2001**, *7*, 306−317.
(32) Gasteiger, J.; Marsili, M. Iterative partial equalization of orbital electronegativity: a rapid access to atomic charges. *Tetrahedron* **1980**, *36*, 3219−3228.

JM050231M